Predicting Defects in Soft Sphere Packings near Jamming Using the Force Network Ensemble

James D. Sartor* and Eric I. Corwin
Department of Physics and Materials Science Institute, University of Oregon, Eugene, Oregon 97403, USA

(Received 8 September 2021; accepted 23 September 2022; published 24 October 2022)

Amorphous systems of soft particles above jamming have more contacts than are needed to achieve mechanical equilibrium. The force network of a granular system with a fixed contact network is thus underdetermined and can be characterized as a random instantiation within the space of the force network ensemble. In this Letter, we show that defect contacts that are not necessary for stability of the system can be uniquely identified by examining the boundaries of this space of allowed force networks. We further show that, for simulations in the near jamming limit, this identification is nearly always correct and that defect contacts are broken under decompression of the system.

DOI: 10.1103/PhysRevLett.129.188001

From crafting swords and arrowheads in antiquity to perusing katanas at the mall today, choosing the available materials with highest strength has always been of critical concern. It is the weak points, and modes of failure, that determine the strength of a material. In polycrystalline materials, these weak points arise from defects in the crystal structure [1]. Early approaches to amorphous systems modeled them as highly defective crystalline systems, but such models fail to capture emergent phenomena [2]. Amorphous systems thus must be treated in their own right; consequently, there exists no obvious definition of a defect. However, "soft spots" can be found, which are locations in which rearrangements are more likely to occur under shear. These were first identified via analysis of the low-frequency quasilocalized vibrational modes [3–6] and have been further explored using machine learning analysis on the local structure [7–15]. While these methods have been effective at identifying rearrangement sites under shear, they have not been applied to systems under decompression, another common failure mode of materials. More importantly, while softness is correlated with structural quantities such as local potential energy and coordination number, these structural properties are not good predictors of rearrangements on their own. Thus softness, while useful as a heuristic, lacks analytic clarity. Additionally, while softness is an excellent predictor of instabilities, it does not predict stable contact network changes (i.e., contact changes that do not result in rearrangements), which comprise the majority of contact network changes [16,17]. Here, we demonstrate a method for identifying defective contacts under decompression asymptotically close to the jamming-unjamming transition. We use the geometry of the force network ensemble to show that in the near-jamming limit there exists only a small and precisely identifiable number of contacts at which any contact network change can occur.

To achieve mechanical stability, any system must have at least as many constraints as degrees of freedom. In a granular system, these constraints are borne by the contacts, and for a d-dimensional system of N frictionless spheres, the minimum number of contacts $N_c^* \sim Nd$ [18]. Any system that possesses more than N_c contacts will have a resultant indeterminacy in its force networks as there must exist multiple linearly independent solutions for force balance. Near jamming, the overlaps (or deformations) between particles are much smaller than the interparticle distances. Because of this separation of scales, the forces in a system can be decoupled from the particle positions, and therefore can be considered to be a random instantiation within the space of the force indeterminacy [19–22]. This is the motivation for the force network ensemble (FNE), which samples all valid force networks in the spring representation of a packing with equal probability.

The rigidity matrix $\mathcal{R}$ represents a granular system as an unstressed spring network by encoding the normalized contact force vectors $\hat{n}_{ij}$ between pairs of particles i and j as

$$\mathcal{R}^{k\gamma}_{\langle ij\rangle} = (\delta^k_j - \delta^k_i)\hat{n}^\gamma_{ij}, \tag{1}$$

where k indexes particles, γ indexes spatial dimensions, and δ is the Kronecker delta [19,23–25]. In periodic boundary conditions, the minimum number of contacts required for stability is [26]

$$N_c^* = Nd - d + 1, \tag{2}$$

and a system with N_c^* contacts will have one stable force network configuration. For each additional contact in excess of N_c^*, the associated unstressed spring network will have an additional linearly independent mechanically

stable force network. These linearly independent force networks are termed "states of self stress" (SSS). These are the left singular vectors of $\mathcal{R}$ associated with the zero singular values of $\mathcal{R}$, i.e., the vectors F_i such that $F_i\mathcal{R} = \vec{0}$. While these SSS contain compressive as well as tensile forces, physical packings of frictionless spheres are constrained to compressive forces. Thus, we consider the FNE to be the set of linear combinations of SSS which contain only non-negative forces.

We previously demonstrated that, by considering the geometric nature of the SSS of a system, one can calculate the volume of the (normalized) force network ensemble and from that the entropy of the force networks [19]. Further contemplation of this geometry leads us to examine the boundaries of this volume, which necessarily include contacts with no stress. These contacts may thus be brought to zero force without breaking the mechanical stability of the system. We primarily focus on systems with exactly two states of self stress (2SSS), which are geometrically confined to have exactly two such boundaries. Each boundary corresponds to a set of contacts (typically each containing exactly one contact), which are unnecessary for mechanical stability of the packing. The breaking of this unnecessary contact results in a packing with only one SSS (1SSS). These boundaries of the volume of allowed force space identify the contacts that may be broken under decompression.

We use pyCudaPacking [27], a GPU-based simulation engine, to generate monodispersed three-dimensional harmonic soft sphere packings. We minimize the packings in periodic boundary conditions using the FIRE minimization algorithm [28]. Using the same methods as in Refs. [29,30], we start with randomly distributed particles at a packing fraction φ far above the jamming packing fraction φ_j and apply a search algorithm to create systems approximately logarithmically spaced in excess packing fraction, $\Delta\varphi = \varphi - \varphi_j$. We generate systems finely spaced in $\Delta\varphi$ (100 steps per decade) to probe the dynamics of the transition from two or more SSS to 1SSS. We continue this process until the system has exactly one state of self stress. We generate datasets of 500 systems at $N = 128$, 1024, and 100 systems at $N = 8192$. We measure the pressure P from the trace of the stress tensor as in Ref. [31] and denote the pressure at which the system reaches 1SSS as P^*.

The space of all normalized linear combinations of SSS is an $N_c - 1$-dimensional space of coefficients. The force network ensemble is the set of coefficients to linear combinations of these SSS for which all forces are non-negative. This can be understood as an "allowed" region in this space of linear combinations of SSS. While force networks within this region are purely compressive, at the boundaries of this region, the load on at least one contact in the system must be precisely zero. In any system with multiple SSS, one can exploit the orthogonality of the SSS to choose the linear combination that yields zero force on any given contact. The imposition of this constraint necessarily reduces N_{SSS}, the number of SSS, by one, and within the context of the force network ensemble is equivalent to breaking a contact. However, with most contacts, this will result in negative forces (i.e., tensile loads) on some of the contacts unless the contact chosen is on the boundary of the allowed volume of force space. We demonstrate this geometrically for a 2SSS system in Fig. 1.

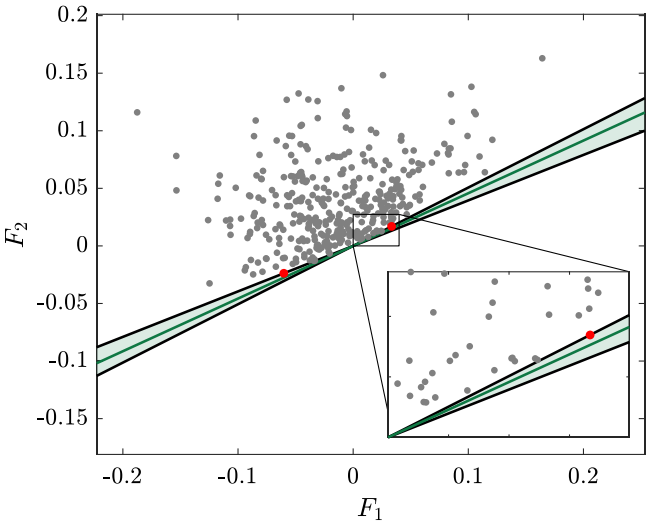

FIG. 1. Scatter plot of the loads on each contact in the two states of self stress F_1 and F_2 (shown with arbitrary rotation) for a typical system ($N = 128$) at 2SSS. Each point represents a contact in the system, with the x coordinate determined by the load in F_1 and the y coordinate determined by the load in F_2 for that contact. Positive values represent compressive loads, and negative values represent tensile loads. A sloped line passing through the origin (at angle α) represents the linear combination $F_1 \sin\alpha + F_2 \cos\alpha$. The load on each contact in this linear combination can be understood as the distance from the line to each point. The black lines represent the two linear combinations of force eigenvectors at the boundary of the allowed region of force space (shaded green), i.e., the set of linear combinations for which all loads are compressive (or zero). These two linear combinations necessarily each bring a different set of contacts to zero force, shown highlighted in red. The green line shows the linear combination of the states of self stress that corresponds to the measured physical forces in the packing. Inset: a region near the origin in greater detail. For a more pedagogical explanation of this manner of visualizing the FNE, see Fig. 1 in [19].

In a 2SSS system, the space of normalized linear combinations of the SSS is a one-dimensional space of rotations, as any stable force configuration f can be described by a mixing angle α such that $f = \sin(\alpha)F_1 + \cos(\alpha)F_2$, where F_1 and F_2 are the linearly independent SSS. Although the physical forces in the packing are instead calculated from the overlaps, they represent a stable force network and as such we are always able to express them with a mixing angle in this way, up to machine

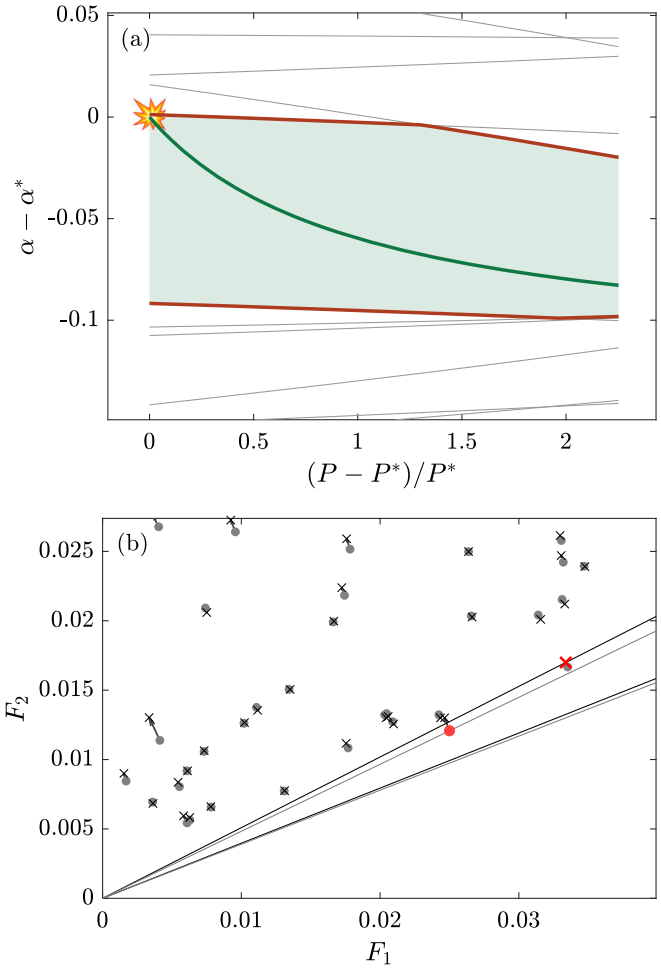

FIG. 2. (a) Evolution of mixing angle representation of the force space under decompression for the system in Fig. 1 over the range of pressures for which the system is at 2SSS. Position in force space is shown as mixing angles $\alpha - \alpha^*$, where α^* is the mixing angle of the system at the contact breaking event. Green shaded region shows all mixing angles for positive-definite force networks. Green line shows the physical forces. Red lines show the boundaries of the force network ensemble. Gray lines show mixing angles that would bring other contacts to zero force. (b) Evolution of the system in force space, shown as in the inset to Fig. 1. The highest and lowest pressures at which the system is at 2SSS are shown as gray circles and black x's respectively, with arrows between them. Breakable contacts on the edge of force space are shown in red.

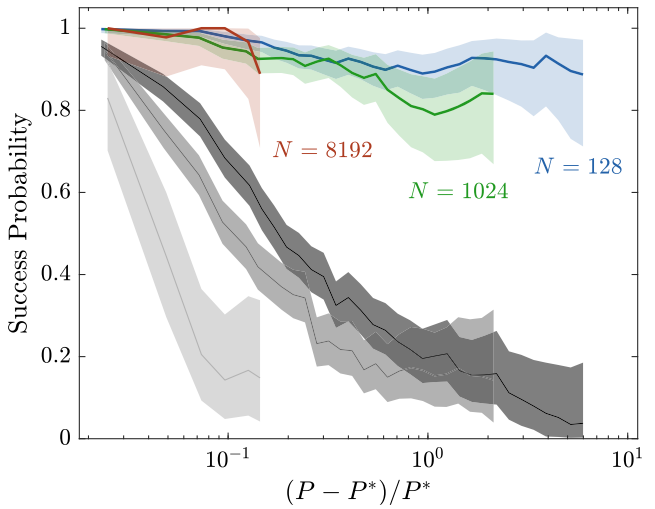

FIG. 3. Probability of predicting contact breaking versus scaled pressure, for systems decompressing from 2SSS to 1SSS. The prediction is counted as a success if one of the two predicted sets of contacts are broken when the system reaches 1SSS. Data shown for FNE predictions in $N = 128$ (blue), 1024 (green), 8192 (red), for pressures at which at least 25 systems remain at 2SSS. The shaded region around each curve shows the 95% confidence interval for the estimation of the probability. Success of the affine response prediction of the smallest two contacts is shown for $N = 128$ (dark gray), 1024 (medium gray), 8192 (light gray).

precision and an overall scale factor. In the intervals between contact changes, we may thus consider the physical forces in the packing as flowing within this space of SSS, which is only gently changing with pressure, as can be seen in Fig. 2(b). As the SSS space is degenerate, there is a free overall rotation in the choice of F_1 and F_2 for each system, which we break by rotating the force points until the bare sum of the loads in F_2 is maximized. This has the effect of reducing the relative motion of the force points during decompression, which we discuss further in the Supplemental Material [32]. In Fig. 2(a), we show the mixing angles that describe the position within this space for the physical forces of a 2SSS system as it decompresses toward $P = P^*$. By following these angles as a system decompresses, we see how the physical forces in the system approach and reach one of the 1SSS states on the boundaries of the 2SSS space. As an example, we can follow the upper red curve in Fig. 2(a) down in pressure toward the contact break, and we see that this system has a kink around $(P - P^*)/P^* \sim 1.3$. This arises from the exchange of the contact that originally formed the boundary of the allowed force space for another, which can be seen graphically in Fig. 2(b). This represents a change in which contacts are considered necessary for stability by the FNE, so for systems in which this occurs, our prediction is accurate only at pressures below that at which the exchange occurs. This interchange of boundary contacts with other contacts that were initially near the boundary is relatively unusual and is the only mechanism by which our prediction fails.

In a 2SSS system, there are always exactly two boundaries on the edge of the force space that correspond to two sets of "breakable contacts." Each of these sets of contacts usually contain just one contact, but sometimes breaking a contact will form a new rattler, all of whose previous contacts must also subsequently break. In such a case, all of these contacts will be found in the set of breakable contacts. In Fig. 3, we show the probability that one of these sets of breakable contacts is in fact broken under decompression

from 2SSS to 1SSS. We find that the contacts predicted by the FNE are strongly predictive ($> 80\%$) over the full range of pressures for which the system has 2SSS. We compare this to the naïve prediction from affine response: if the system were to decompress uniformly, the contact with the smallest overlap, and thus the smallest force magnitude, would break first. Since the FNE predicts two sets of breakable contacts, we instead consider the affine prediction as successful if one of the two contacts with smallest overlap breaks. While affine response is predictive close to the contact breaking event, the predictive power quickly falls to zero at higher pressures.

As shown in Fig. 3, the two breakable contacts are highly predictive for a 2SSS system. At increased pressure, the number of contacts, and thus the dimensionality of the space of normalized SSS, $d_{\mathrm{SSS}} = N_{\mathrm{SSS}} - 1$, increases as well. We examine the scaling of N_{cj}, the number of possible critically jammed systems consistent with the breakage of geometrically allowed subsets of these breakable contacts. At 2SSS, the FNE can be understood as a line that encompasses the set of allowed mixing angles. In this case, $N_{\mathrm{cj}} = 2$, as there are exactly two end points to a line. At 3SSS, the boundaries of the allowed force space are the edges of a polygon, and at higher SSS the facets of a polytope. The vertices of these polytopes represent the predicted critically jammed systems. We find N_{cj} to scale with the dimensionality of the normalized SSS as $\bar{N}_{\mathrm{cj}} \approx 0.64 \times 2.94^{d_{\mathrm{SSS}}}$. For more discussion of N_{cj}, see the Supplemental Material [32].

We predict that N_{cj} critically jammed systems are compatible with the FNE of any system at $>$ 1SSS. In Fig. 4, we show the rate at which one of these predicted critically jammed systems is in fact realized under decompression. We compare our prediction to a naïve prediction from affine response of the N_{cj} critically jammed systems, in which sets of the contacts with the smallest forces break. The strength of our prediction falls with N_{SSS}. For an $N = 1024$ system at 5SSS, we typically predict about 40 sets of four breakable contacts (out of 60×10^{12} possible sets). We find that under decompression one of these sets of four contacts breaks about half of the time. When looking instead at the naïve prediction of the 40 unique sets of size four containing the contacts with smallest loads, we find one of them to correctly identify the actually realized critically jammed system under decompression only $\sim$10% of the time.

Although all predicted force networks within the FNE are necessarily *mechanically* stable (i.e., force balanced), the minima at these points are not necessarily stable equilibria. It has recently been shown that only $\sim$14% of contact change events are irreversible rearrangements (i.e., instabilities), with the remaining $\sim$86% being reversible (i.e., stable) contact network events [16,17]. While our FNE method is able to predict both rearrangements and network events, rearrangement events cascade into additional changes in the contact network. Thus, in addition to the interchange of boundary contacts that can lead to a failed prediction (as illustrated in Fig. 2), systems with $>$ 2SSS may correctly identify a breakable contact which, upon breaking, causes a rearrangement that drastically alters the contact network and thus the force network ensemble. Since only 86% of contact change events are reversible, we expect that each additional contact change predicted can only carry an 86% chance of possibly predicting the next contact. Thus, as the number of SSS (and thus contacts) increases we expect that the success probability for predicting critically jammed systems scales as $\sim 0.86^{d_{\mathrm{SSS}}}$. This predicted scaling is qualitatively similar to the scaling of success probability shown in Fig. 4.

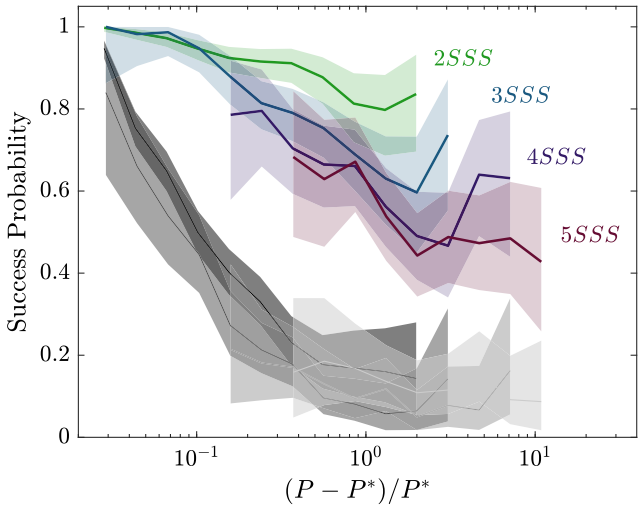

FIG. 4. Probability of correctly predicting contact breaking by FNE versus scaled pressure, for systems of $N = 1024$ particles decompressing from 2, 3, 4, and 5SSS to 1SSS. Colors represent number of states of self stress as indicated. At each pressure, the prediction is counted as a success if one of the N_{cj} predicted sets of contacts are broken when the system reaches 1SSS. As in Fig. 3, data are shown only for pressures at which at least 25 systems remain at the indicated number of SSS. The shaded region around each curve shows the 95% confidence interval for the estimation of the probability. Probability of any of the N_{cj} combinations of the smallest forces in the system breaking is shown in gray, from 2SSS (darkest gray) to 5SSS (lightest gray).

We have shown that the force network ensemble of jammed systems may be used to identify defective contacts that are highly likely to break under decompression. While in spirit these defects can be thought of as analogous to soft spots, we emphasize two key differences here: (1) soft spots identify locations of instabilities, while the force network ensemble identifies locations of both instabilities and stable contact network changes; (2) while soft spots may be identified using just local information, the FNE approach by definition invokes global information. One might wish to use local information to find these defects, and there exists local structure to the force networks when the system

is far from jamming [33]. However, at the jamming point, the system becomes marginal, and as such any change in the contact network impacts the whole force network. Thus, we believe that it would not be possible to identify these defective contacts near jamming without global information.

Open questions remain as to the origin of the scaling of $\bar{N}_{cj}$. Additional future steps include exploring how the physical system chooses which contact to break among the breakable contacts and predicting the values of P^* for individual systems. Another interesting avenue is the search for force network defects in ultrastable systems [34–36], which have more contacts near jamming than random packings, and as such the defects may be delocalized or poorly defined. Since our protocol identifies both stable contact changes and instabilities, a final remaining question is whether these can be differentiated via the force network ensemble, which would provide a more complete picture of the defects within the system.

We thank Varda Hagh, Sean Ridout, Brian Tighe, Rafael Díaz Hernández Rojas, and Peter Morse for valuable discussion and feedback. This work is supported by the Simons Collaboration on Cracking the Glass Problem via Grant No. 454939.

*Corresponding author.
jsartor7@uoregon.edu

[1] G. Taylor, The mechanism of plastic deformation of crystals. Part I.-Theoretical, Proc. R. Soc. A **145**, 362 (1934).
[2] C. P. Goodrich, A. J. Liu, and S. R. Nagel, Solids between the mechanical extremes of order and disorder, Nat. Phys. **10**, 578 (2014).
[3] A. Widmer-Cooper, H. Perry, P. Harrowell, and D. R. Reichman, Irreversible reorganization in a supercooled liquid originates from localized soft modes, Nat. Phys. **4**, 711 (2008).
[4] M. L. Manning and A. J. Liu, Vibrational Modes Identify Soft Spots in a Sheared Disordered Packing, Phys. Rev. Lett. **107**, 108302 (2011).
[5] E. Lerner, G. Düring, and M. Wyart, Low-energy non-linear excitations in sphere packings, Soft Matter **9**, 8252 (2013).
[6] M. Shimada, H. Mizuno, M. Wyart, and A. Ikeda, Spatial structure of quasilocalized vibrations in nearly jammed amorphous solids, Phys. Rev. E **98**, 060901(R) (2018).
[7] E. D. Cubuk, S. S. Schoenholz, J. M. Rieser, B. D. Malone, J. Rottler, D. J. Durian, E. Kaxiras, and A. J. Liu, Identifying Structural Flow Defects in Disordered Solids Using Machine-Learning Methods, Phys. Rev. Lett. **114**, 108001 (2015).
[8] E. D. Cubuk, S. S. Schoenholz, E. Kaxiras, and A. J. Liu, Structural properties of defects in glassy liquids, J. Phys. Chem. B **120**, 6139 (2016).
[9] J. Ding, S. Patinet, M. L. Falk, Y. Cheng, and E. Ma, Soft spots and their structural signature in a metallic glass, Proc. Natl. Acad. Sci. U.S.A. **111**, 14052 (2014).
[10] S. Wijtmans and M. L. Manning, Disentangling defects and sound modes in disordered solids, Soft Matter **13**, 5649 (2017).
[11] S. S. Schoenholz, E. D. Cubuk, D. M. Sussman, E. Kaxiras, and A. J. Liu, A structural approach to relaxation in glassy liquids, Nat. Phys. **12**, 469 (2016).
[12] S. S. Schoenholz, A. J. Liu, R. A. Riggleman, and J. Rottler, Understanding Plastic Deformation in Thermal Glasses from Single-Soft-Spot Dynamics, Phys. Rev. X **4**, 031014 (2014).
[13] D. Richard, M. Ozawa, S. Patinet, E. Stanifer, B. Shang, S. A. Ridout, B. Xu, G. Zhang, P. K. Morse, J.-L. Barrat, L. Berthier, M. L. Falk, P. Guan, A. J. Liu, K. Martens, S. Sastry, D. Vandembroucq, E. Lerner, and M. L. Manning, Predicting plasticity in disordered solids from structural indicators, Phys. Rev. Mater. **4**, 113609 (2020).
[14] J. W. Rocks, S. A. Ridout, and A. J. Liu, Learning-based approach to plasticity in athermal sheared amorphous packings: Improving softness, APL Mater. **9**, 021107 (2021).
[15] S. A. Ridout, J. W. Rocks, and A. J. Liu, Correlation of plastic events with local structure in jammed packings across spatial dimensions, Proc. Natl. Acad. Sci. U.S.A. **119**, e2119006119 (2022).
[16] P. Morse, S. Wijtmans, M. van Deen, M. van Hecke, and M. L. Manning, Differences in plasticity between hard and soft spheres, Phys. Rev. Res. **2**, 023179 (2020).
[17] P. J. Tuckman, K. VanderWerf, Y. Yuan, S. Zhang, J. Zhang, M. D. Shattuck, and C. S. O'Hern, Contact network changes in ordered and disordered disk packings, Soft Matter **16**, 9443 (2020).
[18] J. C. Maxwell, On the calculation of the equilibrium and stiffness of frames., London, Edinburgh, Dublin Philos. Mag. J. Sci. **27**, 294 (1864).
[19] J. D. Sartor and E. I. Corwin, Direct measurement of force configurational entropy in jamming, Phys. Rev. E **101**, 050902 (2020).
[20] J. H. Snoeijer, T. J. H. Vlugt, M. van Hecke, and W. van Saarloos, Force Network Ensemble: A New Approach to Static Granular Matter, Phys. Rev. Lett. **92**, 054302 (2004).
[21] B. P. Tighe, J. H. Snoeijer, T. J. H. Vlugt, and M. van Hecke, The force network ensemble for granular packings, Soft Matter **6**, 2908 (2010).
[22] B. P. Tighe and T. J. H. Vlugt, Stress fluctuations in granular force networks, J. Stat. Mech. (2011) P04002.
[23] W. G. Ellenbroek, V. F. Hagh, A. Kumar, M. Thorpe, and M. van Hecke, Rigidity Loss in Disordered Systems: Three Scenarios, Phys. Rev. Lett. **114**, 135501 (2015).
[24] P. Charbonneau, E. I. Corwin, G. Parisi, and F. Zamponi, Jamming Criticality Revealed by Removing Localized Buckling Excitations, Phys. Rev. Lett. **114**, 125504 (2015).
[25] V. F. Hagh, E. I. Corwin, K. Stephenson, and M. F. Thorpe, A broader view on jamming: From spring networks to circle packings, Soft Matter **15**, 3076 (2019).
[26] C. P. Goodrich, A. J. Liu, and S. R. Nagel, Finite-Size Scaling at the Jamming Transition, Phys. Rev. Lett. **109**, 095704 (2012).

[27] P. Charbonneau, E. I. Corwin, G. Parisi, and F. Zamponi, Universal Microstructure and Mechanical Stability of Jammed Packings, Phys. Rev. Lett. **109**, 205501 (2012).

[28] E. Bitzek, P. Koskinen, F. Gähler, M. Moseler, and P. Gumbsch, Structural Relaxation Made Simple, Phys. Rev. Lett. **97**, 170201 (2006).

[29] J. D. Sartor, S. A. Ridout, and E. I. Corwin, Mean-Field Predictions of Scaling Prefactors Match Low-Dimensional Jammed Packings, Phys. Rev. Lett. **126**, 048001 (2021).

[30] P. K. Morse and E. I. Corwin, Echoes of the Glass Transition in Athermal Soft Spheres, Phys. Rev. Lett. **119**, 118003 (2017).

[31] C. S. O'Hern, L. E. Silbert, A. J. Liu, and S. R. Nagel, Jamming at zero temperature and zero applied stress: The epitome of disorder, Phys. Rev. E **68**, 011306 (2003).

[32] See Supplemental Material at http://link.aps.org/supplemental/10.1103/PhysRevLett.129.188001 for additional details of our methods of predicting breakable contacts and comparing systems, as well as some additional data exploring 1) the scaling of the numbers of breakable contacts and number of critically jammed systems with the number of states of self stress and (2) correlations between breakable contacts.

[33] D. M. Sussman, C. P. Goodrich, and A. J. Liu, Spatial structure of states of self stress in jammed systems, Soft Matter **12**, 3982 (2016).

[34] G. Kapteijns, W. Ji, C. Brito, M. Wyart, and E. Lerner, Fast generation of ultrastable computer glasses by minimization of an augmented potential energy, Phys. Rev. E **99**, 012106 (2019).

[35] V. F. Hagh, S. R. Nagel, A. J. Liu, M. L. Manning, and E. I. Corwin, Transient degrees of freedom and stability, Proc. Natl. Acad. Sci. U.S.A. **119**, e2117622119 (2022).

[36] A. Ninarello, L. Berthier, and D. Coslovich, Models and Algorithms for the Next Generation of Glass Transition Studies, Phys. Rev. X **7**, 021039 (2017).